Quaternary International 430 (2017) 60–70

Contents lists available at ScienceDirect

Quaternary International

journal homepage: www.elsevier.com/locate/quaint

Natural vs. anthropogenic sources supply aeolian dust to the Miaoergou Glacier: Evidence from Sr–Pb isotopes in the eastern Tienshan ice core

Zhiheng Du [a, c, *], Cunde Xiao [a, b, **], Yaping Liu [a], Jiao Yang [a, c], Chuanjin Li [a]

[a] State Key Laboratory of Cryospheric Sciences, Cold and Arid Regions Environmental and Engineering Research Institute, Chinese Academy of Sciences, Lanzhou, Gansu 730000, China
[b] Institute of Climate System, Chinese Academy of Meteorological Science, China Meteorology Administration, Beijing 100081, China
[c] University of Chinese Academy of Science, Beijing 100049, China

ARTICLE INFO

Article history:
Available online 12 December 2015

Keywords:
Eastern Tienshan ice core
Soluble and insoluble dust
Dust source
Sr–Pb isotopic ratios

ABSTRACT

The compositions of Sr and Pb isotopes in the soluble and insoluble dust in six samples from the Miaoergou ice core in eastern Tienshan, China, were measured. The six samples were dated from top to bottom as follows: 2000 AD, 1991 AD, 1983 AD, 1977 AD, 1962 AD and 1958 AD. The $^{87}Sr/^{86}Sr$ ratios in the soluble fraction ranged from 0.709984 to 0.711031. The isotopic ratios of Pb in the soluble and insoluble dust were between 17.962–18.182 and 18.198–18.409 for $^{206}Pb/^{207}Pb$; 15.540–15.606 and 15.560–15.581 for $^{208}Pb/^{207}Pb$; and 37.994–38.173 and 38.179–38.384 for $^{208}Pb/^{204}Pb$, respectively. These isotopic results for insoluble dust allowed us to document the origins of the dust in the Miaoergou Glacier in eastern Tienshan. The major sources of the natural aeolian deposits were the Taklamakan and Gobi deserts. Natural and anthropogenic Pb sources were assessed using a simple ternary model in which deserts, lead ore and coal served as the primary sources of insoluble dust. Lead ore, coal combustion, and the use of leaded gasoline in the surrounding area may represent additional anthropogenic sources of soluble dust. Thus, anthropogenic sources could be further investigated by using the dust-free soluble fractions. The Pb concentration and Pb isotopic compositions from the High Asia ice cores provided distinct evidence of the positive influences of anthropogenic factors associated with industrial development and the prevailing atmospheric circulation patterns in these regions.

1. Introduction

Impurities in snow and ice layers from alpine glaciers and polar ice sheets provide a robust and well-preserved history of atmospheric circulation patterns (Thompson et al., 2000; Ruth et al., 2007; Wu et al., 2013). For example, the mineral dust concentrations (fluxes) in the Antarctica Dome C ice core are correlated with temperature records during glacial periods (Lambert et al., 2008), and the dust record for the Tibet Plateau ice core has been used as a proxy for westerlies (Grigholm et al., 2015). To determine the extent and time frame of global contamination by anthropogenic heavy metals, various investigations have been performed to understand the occurrence of selected metals (Hong et al., 1994, 2012; McConnell and Edwards, 2008; Hur et al., 2013). Several reliable time series have been reconstructed using Pb, Cr, Fe, Rb, Ba, U and Hg based on ice core records (Boutron et al., 1991; Marteel et al., 2008; Jitaru et al., 2009). These results indicate the history of human interferences in the environmental mobilization of these elements at regional to global scales.

Asian dust is the second largest source of dust on Earth. Observational evidence has suggested that dust originating from East Asia has a significant global influence (Biscaye et al., 1997; Bory et al., 2002, 2003; Uno et al., 2009; Maher et al., 2010; Takahashi et al., 2011). Therefore, specific intrinsic tracers that can estimate the environmental characteristics of natural emissions and anthropogenic effects are necessary. In recent decades, the stable-

* Corresponding author. State Key Laboratory of Cryospheric Sciences, Cold and Arid Regions Environmental and Engineering Research Institute, Chinese Academy of Sciences, Lanzhou, Gansu 730000, China.
** Corresponding author. State Key Laboratory of Cryospheric Sciences, Cold and Arid Regions Environmental and Engineering Research Institute, Chinese Academy of Sciences, Lanzhou, Gansu 730000, China.
E-mail addresses: duzhiheng10@163.com (Z. Du), cdxiao@lzb.ac.cn (C. Xiao).

http://dx.doi.org/10.1016/j.quaint.2015.11.069
1040-6182/

isotopic ratios of lead (Pb) and strontium (Sr) isotopes have been used as naturally occurring tracers to identify dust provenances and to provide insight regarding the pathways of pollution transport from a source to a receptor in association with the atmospheric circulation patterns in ice core studies (Rosman et al., 1993; Biscaye et al., 1997; Grousset and Biscaye, 2005; Burton et al., 2007; Osterberg et al., 2008; McConnell and Edwards, 2008; Vallelonga et al., 2010; Lee et al., 2011; Gross et al., 2012; Delmonte et al., 2013; Bory et al., 2014).

Miaoergou Glacier (43°03′19″N, 94°19′21″E, 4512 m a.s.l.) is located in the eastern Tienshan, surrounded by the Taklamakan and Gobi deserts. Because the mountains extend well into the troposphere, the ice cores from this region can provide a unique medium for studying the characteristics of well-mixed low- and mid-tropospheric Asian dust (Nagatsuka et al., 2010; Wu et al., 2010; Xu et al., 2012; Du et al., 2015). Previous studies have investigated the alpine ice cores surrounding the Asian desert rim, and most of the Sr-Nd-Pb isotope measurements were collected using bulk snow or ice samples (Wu et al., 2010; Yu et al., 2013). However, data regarding the origin of radiogenic species in the soluble fraction of the ice cores in this region do not exist. These data are required for interpreting the dissolved chemical species signals of ice cores and can serve as a complementary proxy for atmospheric data by tracing the sources of these dissolved elements (Lupker et al., 2010). In this study, the compositions of Sr and Pb isotopes in dirty layers in the Miaoergou ice core were measured insoluble and insoluble dust to identify the natural dust provenances and anthropogenic effects.

2. Sample treatment and measurement

2.1. Sampling treatment

Miaoergou Glacier lies to the north of Hami Basin, which extends southward from the Karlik Mountains (Fig. 1). In 2005, two ice cores (~9.4 cm in diameter) to bedrock (58.7 m and 57.6 m in length for Core 1 and Core 2, respectively) were obtained from a dome on the Miaoergou Glacier. The Core 1 was split axially into two equal halves. One half was used in this study and Du et al. (2015), and the other was archived. The difference in length of two ice cores is negligible, primarily due to the bottom topography of glacier. Therefore, Core 1 was dated (Liu et al., 2011). The net accumulation rate of the Miaoergou glacier is 20 cm ice equivalent/year (Li et al., 2007a). Therefore, 6 subsamples were collected at intervals of approximately 20–30 cm so that the time span of each subsample was approximately one or two years. Du et al. (2015) described the environmental setting and climatic characteristics of the study site. The decontaminated ice samples were melted at 20 °C under clean room conditions using a class 100 laminar flow bench. Next, the insoluble dust in the ice core was extracted using low protein adsorption hydrophilic polytetrafluoroethylene (PTFE, Whatman) membrane filters (Millipore Corporation, with a diameter of 47 mm and pore size of 0.2 μm). Acid-cleaned low density polyethylene (LDPE) bottles were used to collect the filtrate, which was defined as soluble dust in this study (Table 1). The volume of ice samples varies from 187 to 250 ml, while the insoluble dust mass in the 6 subsamples range from 16 to 45 mg.

The depths of our six subsamples are shown in Table 1. The six samples were dated from top to bottom as follows: 2000 AD, 1991 AD, 1983 AD, 1977 AD, 1962 AD and 1958 AD, yielding an estimated dating uncertainty of ±1 year (Liu et al., 2011).

2.2. Measurements

The filters used to collect insoluble dust were digested in ultrapure nitric acid (HNO_3), hydrofluoric acid (HF) and perchloric acid ($HClO_4$) at temperatures of 160–180 °C in PTFE screw-top bombs. In this study, all the solutions were made using double distilled water at the Analytical Laboratory at the Beijing Research Institute of Uranium Geology (ALBRIUG). The detailed digestion method can be found in the study of Du et al. (2015). Blank filters (collecting insoluble dust) and filtrate (collecting soluble dust) were processed similarly. Then, the Sr and Pb concentrations were measured using inductively coupled plasma mass spectrometry (ELEMENT XR, Thermo Elemental Corporation). The results showed that the Sr and Pb concentrations in the blank filter were all less than 1%, while these concentrations in the filtrate were all less than 5%. The collected insoluble dust was dissolved in 6 ml (1:1) of HNO_3 + 1 ml HF + 0.1 ml $HClO_4$ at temperatures of 160–180 °C in PTFE screw-top bombs before conducting thermal ionization mass spectrometry (TIMS) analysis. The measurement process has been described in previous studies (Wu et al., 2010; Yu et al., 2013). Because the Sr and Pb concentrations in the soluble dust are very low, the instrumental analyses must be conducted in a clean room. First, approximately 180–250 ml of the filtrate was passed through a 0.2 μm filter (PTFE, Whatman). Second, the filtrate was poured into a 500 ml beaker and dried in an ultra-clean bench (class 100). The measurement method of Sr–Pb isotopes in the soluble dust were the same as those of the insoluble dust. The TIMS measurements of the Sr–Pb isotopes were carried out at the Analytical Laboratory at ALBRIUG using an IsoProbe-T spectrometer (GV Corporation). The Pb and Sr isotope measurements are briefly outlined in this section. First, Pb was separated using a 100–200 mesh AG1 X8 anion exchange resin (subsamples were loaded in 0.5 N HBr and Pb was eluted with 6 N HCl). Second, Sr was purified using a standard cation-exchange procedure (φ0.5 cm × 15 cm, AG50 WX8 100–200 mesh) and loaded in 0.5 N HCl. Then, Sr was eluted with 2.5 N HCl. The Pb isotopes were measured using a single Re ribbon with a silica gel emitter in static multicollection mode. To optimize the instrument accuracy, the isotope standard samples of NBS 987 strontium and NBS981 lead (2σ, n = 10) were used in this study, respectively. The $^{208}Pb/^{206}Pb$, $^{207}Pb/^{206}Pb$ and $^{204}Pb/^{206}Pb$ ratios of NBS 981 lead isotope standard were 0.710229 ± 15, 0.914338 ± 7 and 0.0591107 ± 2, respectively. The Sr isotopes were loaded onto single Re filaments and a Ta activator in static multicollection mode. The data were corrected for internal mass biases to $^{86}Sr/^{88}Sr = 0.1194$, and the $^{87}Sr/^{86}Sr$ ratio NBS 987 strontium isotope standard (2σ, n = 10) was 0.710250 ± 7, with a recommended value of 0.710248. The analytical blank was <100 pg for Pb and <200 pg for Sr.

3. Results and discussion

3.1. Pb concentrations record for the different ice cores

The Pb concentrations exhibited significant temporal variations that ranged from 29.7 to 19471.0 ng/l over the period 1953–2004 AD (Liu et al., 2011). A significant increase in the Pb concentrations occurred from 1975 to 1985 AD in the Miaoergou ice core, and another peak occurred in the 1990s (Fig. 2). Similar results were recorded in the Muztagata ice core (75°06′E, 38°17′N), which was obtained from eastern Pamirs and located in the border of Tajikistan, Kyrgyzstan and Kazakhstan in Central Asia (Li et al., 2006). Fig. 2 reveals that the Pb concentrations exist an increase trend from 1955 to 1993 AD, with two Pb concentration peaks in 1980s and 1990s (Li et al., 2006). The exhibited Pb concentrations from Belukha ice core (49°48′N, 86°34′E, 4062 m a.s.l.) were significantly enhanced during the period 1935–1995 AD and

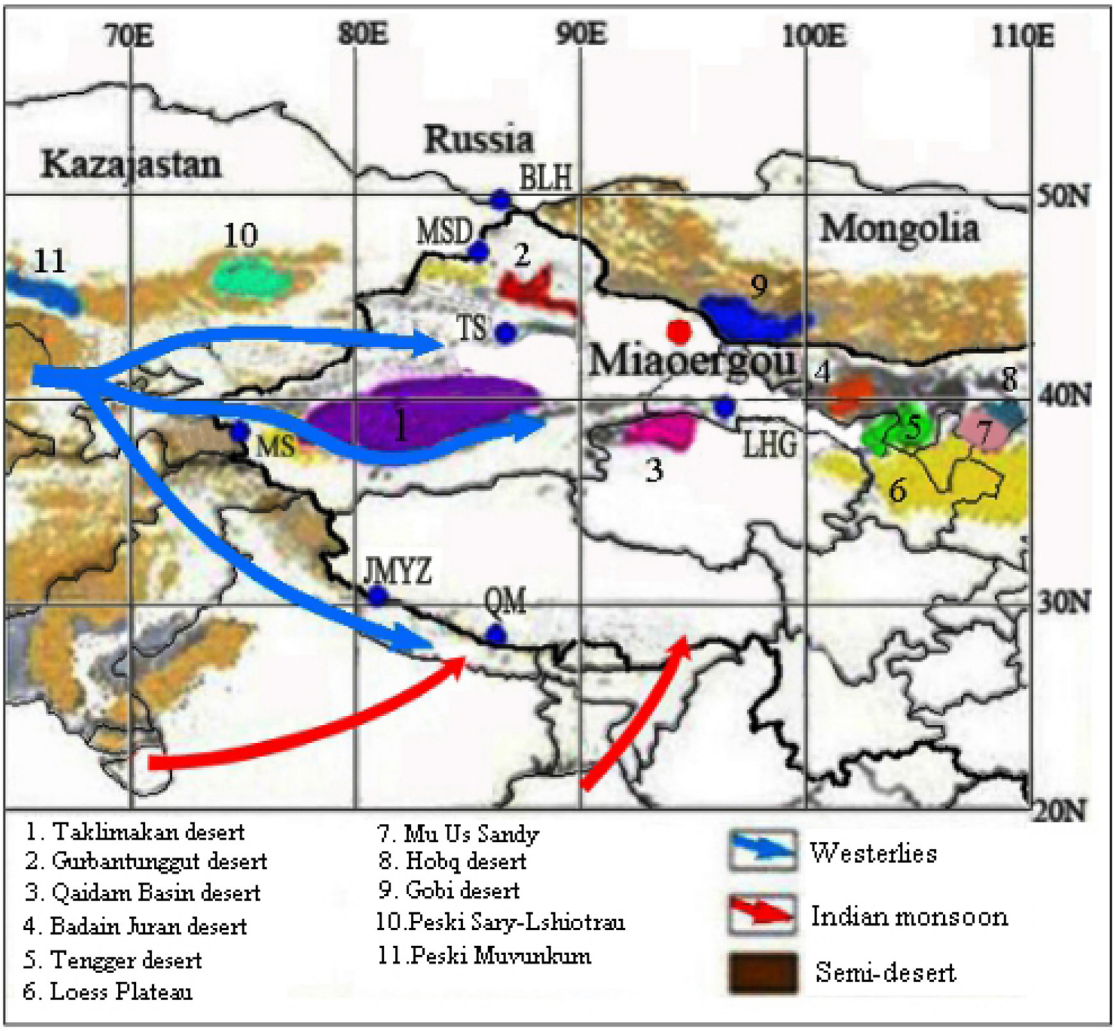

Fig. 1. Location map of the Miaoergou Glacier, ice core and snowpit sampling sites (BLH:Belukha Glacier, MSD:Musidao Glacier, TS:Tienshan NO.1 Glacier, MS: Muztagata Glacier, JMYZ: JiemaYangzong Glacier, QM: East Rongbuk Glacier) and the distribution of deserts in western China.

peaked in the 1970s, this peaked responses to the Europe Pb emission in past 50 years (Von et al., 2003; Eichler et al., 2012). However, the data for the East Rongbuk ice core, which was obtained south of the Tibet Plateau, contained trace metals before ~1953 AD that were controlled by mineral dust inputs, with no discernible volcanic or anthropogenic contributions. Significant increases in the concentrations and crustal enrichment factors were observed from the 1970s onward that abruptly increased during the period 1990–1996 AD (Lee et al., 2011; Hong et al., 2012; Burn-Nunes et al., 2014).

In this study, we cannot reconstruct the Pb histories before the 1950s for Miaoergou and Muztagata ice cores, but there exists a

Table 1
Sr and Pb isotope ratios for soluble dust and insoluble dust in the Miaoergou ice core.

Age (AD)	Depth (cm)	Volume (ml)	Type	$^{87}Sr/^{86}Sr$	2σ	$^{208}Pb/^{204}Pb$	2σ	$^{207}Pb/^{204}Pb$	2σ	$^{206}Pb/^{204}Pb$	2σ
2000	90–120 cm	210	Soluble Dust	0.711031	0.000012	38.034	0.033	15.554	0.014	18.088	0.016
			Insoluble Dust	0.718958[a]	0.000009	38.384	0.004	15.578	0.002	18.409	0.002
1991	332–360	187	Soluble Dust	0.710308	0.000018	38.054	0.013	15.549	0.005	17.971	0.006
			Insoluble Dust	0.717025[a]	0.00001	38.179	0.003	15.571	0.001	18.198	0.002
1983	558–596	187	Soluble Dust	0.710651	0.000013	38.22	0.033	15.572	0.013	18.182	0.015
			Insoluble Dust	0.717455[a]	0.000014	38.40	0.007	15.579	0.003	18.394	0.003
1977	731–755	250	Soluble Dust	0.710392	0.000016	37.994	0.06	15.57	0.025	17.979	0.029
			Insoluble Dust	0.718065[a]	0.000013	38.288	0.005	15.569	0.002	18.352	0.002
1962	1265–1293	250	Soluble Dust	0.710336	0.000012	37.999	0.039	15.54	0.016	17.962	0.018
			Insoluble Dust	0.718013[a]	0.000011	38.166	0.005	15.56	0.002	18.258	0.002
1958	1508–1533	190	Soluble Dust	0.709984	0.000016	38.173	0.053	15.606	0.022	18.132	0.025
			Insoluble Dust	0.718571[a]	0.000012	38.34	0.006	15.581	0.003	18.298	0.003

[a] Stable Sr isotope data of insoluble dust from Du et al. (2015).

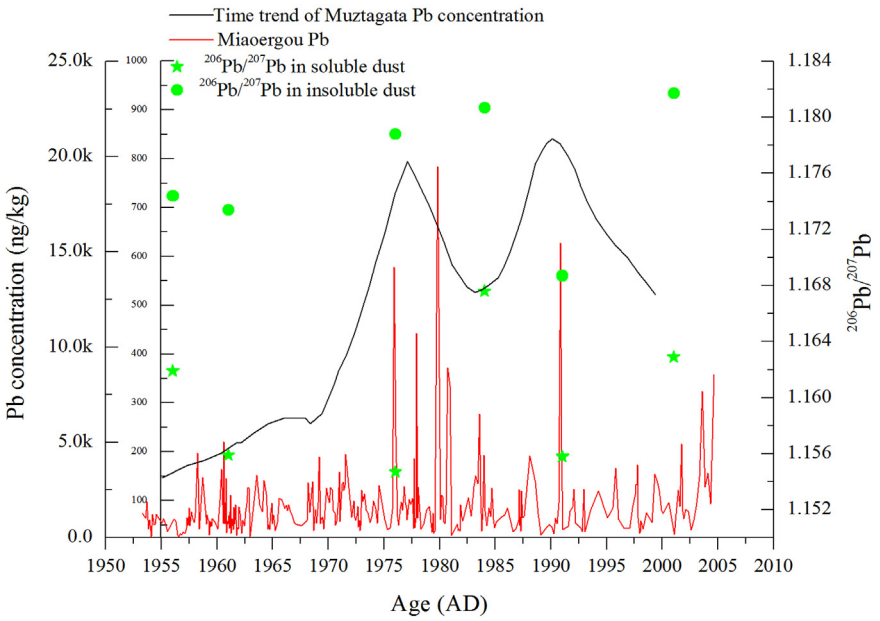

Fig. 2. Concentration record for Pb in the Miaoergou and Muztagata ice cores (Li et al., 2006; Liu et al., 2011) and the Pb isotopic ratios for the insoluble dust and soluble dust fractions.

significant increasing trend during the 1970s and the 1980s (Fig. 2). Pb emission in China distinctly and significantly increased from the 1990s (Fig. 3). Therefore, the variations in the spatial distribution of the ice cores in Tibetan Plateau (TP), Altai and Tienshan are indicative of the temporal variations in industrialization across South Asia, Central Asia and Europe (Li et al., 2006; Eichler et al., 2012; Burn-Nunes et al., 2014).

In 1997, the Chinese government began to phase out leaded gasoline and decrease Pb emissions (Qin, 2010). However, the Pb concentrations in the Miaoergou ice core have increased since 2000 compared with the concentrations observed in the 1980s (Fig. 2). Relatively high Pb concentrations between 1997 and 2002 were also observed in the East Rongbuk ice core (Lee et al., 2011). This phenomenon was also demonstrated in Xiamen, China, in which the annual Pb concentrations in aerosol particles in 2003 increased by approximately 12% compared with those measured between 1991 and 1993 (Zhu et al., 2010). As shown in Fig. 3, this increase was probably due to an increase in coal combustion and automobile production in China (Liu and Zhao, 2006; Li et al., 2006; Qin, 2010; Li et al., 2012). This finding indicates that the Pb concentrations continued to increase after 2000, which was when reform and openness policies were instituted in China.

3.2. Variations in the isotopic compositions of Sr and Pb

Minerals and rocks have distinct Sr and Pb ratios. Because of the extremely long half-lives of radioactive parents, these tracers can be considered as “conservative” fingerprints when applied to

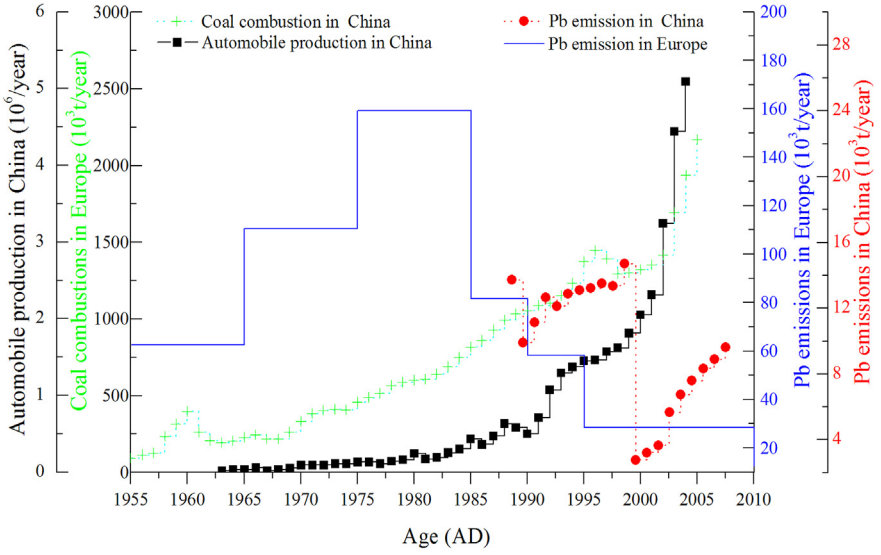

Fig. 3. Historical coal and Pb emission estimates for different regions. The Pb emission data were obtained from Von Storch et al. (2003) and Li et al. (2012), Liu and Zhao. (2006) and the coal combustion data were acquired from Qin (2010).

studies conducted over short periods and during transport in the atmosphere or after deposition as sediments (Grousset and Biscaye, 2005). Previously, researchers evaluated source regions according to geochemical characteristics by extracting dust from Asian mountain glaciers (Wu et al., 2010; Xu et al., 2012; Yu et al., 2013). However, few studies have focused on the composition of the dust-free soluble fraction of ice cores by investigating the isotopic compositions of Sr and Pb (Lupker et al., 2010). The average $^{87}Sr/^{86}Sr$ ratio in the soluble fraction of the Miaoergou ice core was 0.710450 (ranging from 0.709984 to 0.711031), while of ratio in the insoluble dust fraction was 0.718015 (ranged from 0.717025 to 0.718958, Du et al., 2015). The $^{87}Sr/^{86}Sr$ ratios exhibited similar variation trends in the soluble dust and insoluble dust fractions. The ratios for the insoluble dust fraction were substantially higher than those for the soluble dust fraction (Table 1).

^{204}Pb provides a "benchmark" for gauging the relative abundance of the remaining Pb isotopes. Both natural and anthropogenic Pb isotope tracer series exist (Grousset and Biscaye, 2005). The former was obtained from tracing the Aeolian sources (Sun and Zhu, 2010), while the latter utilizes the Pb isotope compositions of anthropogenic pollutants (Lee et al., 2011). The compositions of the soluble dust and insoluble dust fractions in the Miaoergou ice core exhibited the following ranges of Pb isotope ratios: 17.962–18.182 and 18.198–18.409 for $^{206}Pb/^{204}Pb$, 15.540–15.606 and 15.560–15.581 for $^{207}Pb/^{204}Pb$, and 37.994–38.173 and 38.179–38.384 for $^{208}Pb/^{204}Pb$, respectively (Table 1). The soluble Pb data can be compared with snow and ice results from Central Asia glaciers (Yu et al., 2013). The $^{206}Pb/^{207}Pb$ ratios of the soluble dust and insoluble dust fractions followed similar trends. The ratios of the insoluble dust fraction were significantly higher than those of the soluble dust fraction (Fig. 2).

3.3. Evidence of natural vs. anthropogenic Sr and Pb inputs to the Miaoergou ice core

Leaching experiments for the loess from the Chinese Loess Plateau revealed identical $^{87}Sr/^{86}Sr$ ratios for water and HOAc-soluble minerals (Yokoo et al., 2004). Nagatsuka et al. (2010) demonstrated this phenomenon using surface dust from Ürümqi Glacier No. 1 (located on the eastern side of the Tienshan). The $^{87}Sr/^{86}Sr$ ratios for the insoluble dust fraction in the ice core were comparable with the $^{87}Sr/^{86}Sr$ ratios of loess and Gobi samples. However, there were only two samples from the loess source (Biscaye et al., 1997; Widory et al., 2010). Therefore, it requires further demonstrate investigation in future. The $^{87}Sr/^{86}Sr$ and $^{206}Pb/^{207}Pb$ ratios for the soluble fraction in the Miaoergou ice core were similar to those for Chinese coal combustion and cement factories (Fig. 4).

The Sr isotope ratios for the soluble fraction in the Miaoergou ice core were higher than the Sr isotope ratios for the soluble fraction in seawater (0.70917, Dia et al., 1992), which indicates a contribution from at least one radiogenic Sr source. The Miaoergou Glacier is located in arid and semi-arid areas of northwestern China with sparse native vegetation and snow accumulation occurring during the winter and spring. Consequently, plants are an unlikely primary source of Sr in this region. The $^{87}Sr/^{86}Sr$ ratios in water-soluble sands from the Taklamakan desert ranged from 0.710902 to 0.711906 (Nakano et al., 2004), these results are similar with the data as presented in this study (Table 1). Viewed from the topographic characteristics, the Miaoergou Glacier is located along the northeastern edge of the Taklamakan desert (Fig. 1), therefore, it could be a natural source of dust for the glacier. The present study further supports our previous observation (Du et al., 2015).

The second non-sea salt end-member is a probable anthropogenic input. Higher trace metal concentrations were recorded in Ürümqi Glacier No. 1 in eastern Tienshan (Li et al., 2007b). The pollutants from fossil fuel combustion, coal and other fossil fuels are extensively applied for urban heating during late autumn and winter (Li et al., 2007b). Previously, the $^{87}Sr/^{86}Sr$ ratio in water-soluble sands from Ürümqi City, which is approximately 600 km from Miaoergou Glacier, was 0.709510 (Nakano et al., 2004). This result shows the atmospheric pollutants from Ürümqi City may be transported along prevailing westerlies and with low-level regional atmospheric circulation and then their deposit in eastern Tienshan. Data from previous studies have suggested that the $^{87}Sr/^{86}Sr$ ratio ranges between 0.7083 and 0.7335 for urban heating and between 0.7097 and 0.7100 for incinerators in the Parisian (France) atmosphere (Negrel et al., 2007). Although no data are available for western Chinese cities, the $^{87}Sr/^{86}Sr$ ratios for aerosol particles (Fig. 4) range between 0.708970 and 0.709492 for coal combustion and between 0.709963 and 0.712064 for cement factories and smelting in Beijing (Widory et al., 2010). These Sr isotopic ratios for anthropogenic pollution (including urban heating and incinerators) may overlap with the Aeolian dust ratios (Taklamakan desert), but the Sr isotope ratios for the soluble dust fraction are similar to the ratios observed for anthropogenic pollution.

The $^{206}Pb/^{207}Pb$ ratios in the soluble fraction in the Miaoergou subsamples (1977 AD and 1991 AD) were substantially less radiogenic, whereas the Pb concentrations in Miaoergou ice core reach maximum values for the two subsamples. Although a few Pb isotopic data in this study, the composite record of lead $^{206}Pb/^{207}Pb$ isotopic ratios showed that there are coincident with similar gradual changes in Pb concentration (Fig. 2). Particularly, the $^{206}Pb/^{207}Pb$ ratios in the soluble fraction support the idea that an additional unradiogenic Pb-rich end-member or at least an anthropogenic Pb-rich end-member is an influential factor (Fig. 4). These results may imply that the Sr and Pb isotopes in the soluble fraction contain more anthropogenic information and are consistent with anthropogenic sources, which are more radiogenic. Conversely, these two isotopes in the insoluble dust fraction indicate natural Aeolian dust/desert signals.

Because the atmosphere transport pattern over eastern Tienshan is characterized by a predominantly westerly flow along the Pamirs and Tienshan Mountains throughout the year, an impetus for Aeolian dust transportation is prevalent (Fig. 5). The westerlies are split into three distinct branches due to forcing induced by the TP (Yao et al., 2012). The two northern branches influence the Tienshan region, and the wind speeds during spring and summer reach maximum and minimum values at 700 mb (Fig. 5). The air masses from East Asia may weaken the westerlies during the summer, and air mass channels exist between the Halikun (Miaoer Glacier) and Barkol Mountains. Therefore, the air masses from the north are deflected into this region. Particularly, sandstorms frequently occur during the winter and spring. This phenomenon is also confirmed by the wind vectors and circulation patterns over western China (Fig. 5). These meteorological and topography features provide aeolian dust transport conditions for this region.

3.4. Comparison of Sr–Pb isotopes data with alpine and Greenland snow and ice cores

Yu et al. (2013) used cluster statistics to study Pb isotope data from mountain glaciers in western China and identified four similar and distinct groups. However, to emphasis the characteristics of climate systems, the spatial distributions of the glaciers and the Pb isotopic ratios (Figs. 1, 5 and 6), three distinct groups were determined in this study. Group 1 consists of samples from the southern TP, including the East Rongbuk and JiemaYangzong glaciers, which are located along the northern slope of the Himalayas and have high $^{206}Pb/^{207}Pb$ ratios (average of 1.1834).

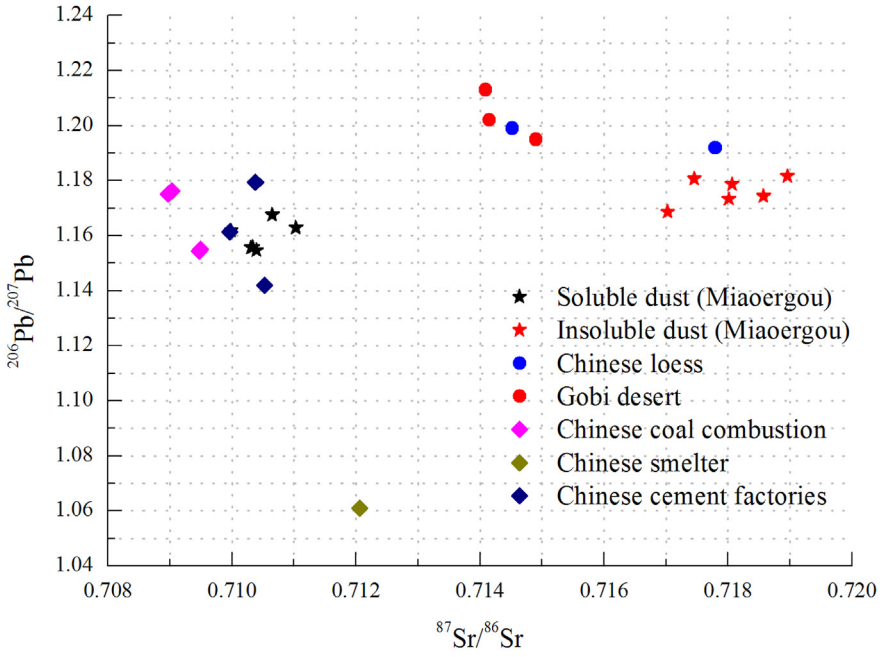

Fig. 4. $^{87}Sr/^{86}Sr$ and $^{207}Pb/^{206}Pb$ ratios for the soluble and insoluble dust fractions in the Miaoergou ice core. The data for the Gobi desert were obtained from Biscaye et al. (1997). Data for the Chinese loess, coal combustion, smelter, and cement factories were acquired from Widory et al. (2010).

Group 2 consists of samples from the Muztagata, Tienshan No. 1, and Laohugou glaciers, which are located near East Asian deserts. The mean $^{206}Pb/^{207}Pb$ ratio in the Muztagata, Tianshan and Laohugou snowpits is 1.1801. Group 3 consists of samples from Musidao Glacier, which is located on the northern boundary of western China (Fig. 1) and has a lower $^{206}Pb/^{207}Pb$ ratio (average of 1.1616). The lead isotopic ratios followed three patterns that were consistent with the atmospheric circulation pattern (northern, central and southern westerlies) and the glacier distribution. These results provide information regarding the sources of Pb in

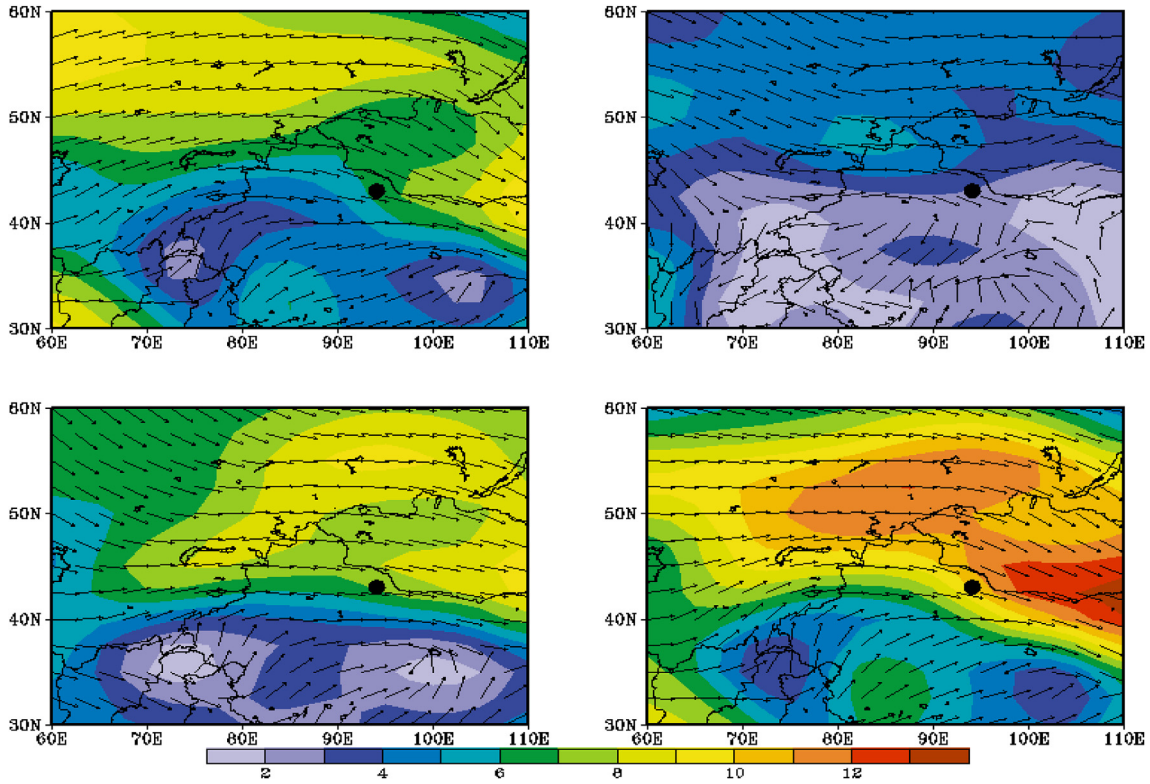

Fig. 5. Seasonal average wind vectors (m/sec) at 700 mb from 1971 to 2000 based on the NCEP/NCAR reanalysis. Spring = JFM, Summer = JJA, Autumn = SON, Winter = DJF. The location of Miaoergou is noted with a black circle.

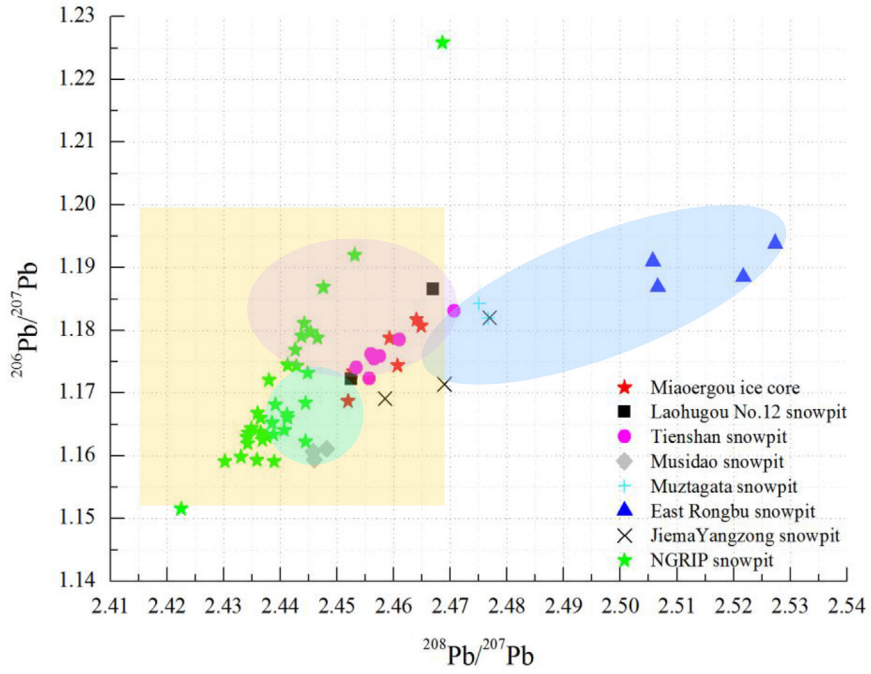

Fig. 6. Comparison of the Pb isotopic Miaoergou insoluble dust results with the Pb isotopic compositions of the other snowpits from Laohugou NO.12, Tienshan NO.1, Musidao, Muztagata (Yu et al., 2013), and NGRIP (Bory et al., 2013).

the snow and ice, which are controlled by climatic and environmental factors.

For group 1 glaciers, the East Rongbuk and JiemaYangzong glaciers are located on the southern TP. The topographic characteristics of this region are distinct from the northern TP. The elevations of the two glaciers are high, and the transport of the aeolian dust from the northern slope of the TP to these regions is difficult. Recent results have demonstrated that air pollutants from the lowlands of South Asia can be transported across the Himalayas via the mountain/valley wind system (Cong et al., 2015). The glaciers of Group 2 are located west of the Taklamakan desert. Aeolian dust, which frequently occurs in this region, is deposited on the surfaces of these sparsely populated and remote glaciers (e.g., Muztagata Glacier) via dry and wet deposition. The Tienshan No. 1 and Miaoergou glaciers are located northeast of the Taklamakan desert and near Ürümqi City, which is the largest population centre in western China. The Laohugou Glacier is located east of the Taklamakan desert and adjacent to Dunhuang City. Previous studies have shown that the chemical ions in the aerosol particles obtained from Laohugou Glacier indicate that the anthropogenic aerosols originated from low-elevation urban areas, including Dunhuang City (Xu et al., 2014). The $^{206}Pb/^{207}Pb$ ratios for these three glaciers are also comparable with the $^{206}Pb/^{207}Pb$ ratios from Chinese coal combustion (1.156–1.200) and indicate the emissions of anthropogenic lead-based substances into the atmosphere in these regions. The Musidao Glacier of Group 3 is located near Belukha Glacier, the mean $^{206}Pb/^{207}Pb$ ratio in the Belukha ice core from 1935 to 1995 AD is 1.153, which is similar to the value obtained for the Musidao snowpit (1.1616). Therefore, similar anthropogenic sources originating from lead ore mining in Altai and industrial emissions in Russia and Eastern Europe existed for both glaciers (Eichle et al., 2012).

By applying the geochemical characteristics of the aeolian mineral dust recorded in Greenland ice cores, the results had demonstrated the dust for Greenland ice sheet originated from the Gobi and TakliMakan desert during the last glacial period (Svensson et al., 2000; Ruth et al., 2007). This result indicates a direct link between the Asian mountain and Greenland ice cores. The average $^{87}Sr/^{86}Sr$ ratio in the soluble fraction of the Dye-3 ice core was 0.710450, while the ratios in the insoluble dust fraction ranged from 0.712406 to 0.720226 (Lupker et al., 2010). The small variations in the $^{87}Sr/^{86}Sr$ ratio between the Miaoergou and Greenland ice cores indicated that a common dust source exists for the two regions. More importantly, these variations indicated similarities between the two ice cores and demonstrated that Asian deserts are likely the main source of aeolian dust for the Greenland ice sheet (Biscaye et al., 1997; Bory et al., 2002, 2003; Burton et al., 2007). The compositions of Pb isotopes in the soluble fraction in the Miaoergou ice core were similar to those observed in the NGRIP snowpits (Fig. 6). Bory et al. (2014) had indicated that Chinese aerosols account for a substantial and growing fraction of the insoluble anthropogenic Pb that has been deposited in central Greenland over the last few decades of the twentieth century. These results suggest that aeolian dust and anthropogenic Pb from East Asia are transported to Greenland.

3.5. Estimation of Natural and anthropogenic contributions to the Miaoergou ice core

Many studies have noted that the geochemical characteristics of background Pb usually yield high $^{206}Pb/^{207}Pb$ ratios, while the Pb from recent industrial sources yields low $^{206}Pb/^{207}Pb$ ratios (Bollhöefer and Rosman, 2002). The East Rongbuk ice core from the Himalayas showed that the isotopic signal of the regional natural background Pb (~1.20 for $^{206}Pb/^{207}Pb$) in the central Himalayas. The Pb concentration significantly increased, and lower $^{206}Pb/^{207}Pb$ ratios were present in the 1970s (Hong et al., 2009; Kaspari et al., 2009; Lee et al., 2011; Burn-Nunes et al., 2014). The $^{206}Pb/^{207}Pb$ ratios from Belukha ice core were significantly enhanced during the period 1935–1995 AD due to the use of Pb additives in Russian gasoline that was mined in the Rudny Altai (Eichle et al., 2012). In this study, the oldest subsamples were dated 1956 AD (Table 1),

potentially due to increasing anthropogenic influence. Therefore, studies should not only consider mineral dust inputs but also anthropogenic effects. To infer the spatial changes in Pb sources, we compared the Pb isotopic ratios in this study with those of the mineral dust from potential source areas (PSAs) and anthropogenic sources from coal combustion, lead ore and leaded gasoline by using a three-isotope plot (Fig. 7).

The Aeolian dust samples from the Taklamakan and Gobi deserts have $^{206}Pb/^{207}Pb$ ratios of 1.187–1.209 and 1.195–1.203, respectively (Biscaye et al., 1997; Li, 2007; Ferrat et al., 2012; Bory et al., 2014). These ranges correspond with the data obtained for Miaoergou insoluble dust, which suggests the presence of natural Aeolian dust sources. The $^{206}Pb/^{207}Pb$ ratios of southern Tienshan and Rudny Altai lead ores range from 1.147 to 1.148 and from 1.139 to 1.156, respectively, which are similar to the ratios that were obtained for the soluble fraction in this study (Mukai et al., 2001; Zhang et al., 2010). The Tienshan Mountains are considered one of the most important metallogenic regions in China, and the geologic characteristics of this region are beneficial for mining Pb and Zn mineral deposits. In recent decades, Pb ore mining has increased (Bollhöfer and Rosman, 2000; Ding et al., 2010). The Altai region has been subject to mining activities since the Bronze Age (Grushin et al., 2009). In Rudny Altai, vast polymetallic deposits containing massive Pb, Cu, Zn, Au, Ag, and Fe sulphide ores were discovered within an area of approximately 30000–50000 km^2 (Farmer and Farmer, 2000; D'yachkov et al., 2009). The $^{206}Pb/^{207}Pb$ ratios for Chinese coal combustion range from 1.156 to 1.200 (Mukai et al., 1993; Chen et al., 2005). The Zhundong coalfield is a very large coal deposit (164 Gt of coal reserves) located in the eastern coal-bearing area of the Junggar basin, which is within the Xinjiang autonomous region, and is currently under exploration and is expected to be an important coal mining resource in western China (Zhou et al., 2010). Urumqi, the capital city of Xinjiang, is one of the most polluted cities in the world. Coalfield fires are surface fires that occur in seams and can occur in open-pit mines. The coal mine fires at private and government mines include underground and surface fires that emit significant Pb into the atmosphere (Stracher and Taylor, 2004; Diaz-Somoano et al., 2009). The gasoline-related (including vehicle exhaust particles and gasoline samples) $^{206}Pb/^{207}Pb$ ratio for Shanghai ranges from 1.120 to 1.139, and the average $^{207}Pb/^{206}Pb$ ratio of leaded gasoline is 1.143 in Russia (Zheng et al., 2004; Eichler et al., 2012). Although leaded gasoline has been phased out in recent decades, coal emissions and automobile production have continuously increased in recent years, which have potentially contributed to Pb pollution in this region. These results indicate that the Pb isotope ratio is derived from anthropogenic sources that may change the Pb isotopic composition. For the Miaoergou Glacier, the anthropogenic sources of Pb are primarily derived from the surrounding lead ore, Chinese coal combustion, and leaded gasoline.

The Pb isotope ratios in the insoluble dust fraction of the Miaoergou ice core are similar to those in desert sources. The soluble dust primarily originates from anthropogenic sources, including lead ore, Chinese coal, leaded gasoline, and smelter and cement factories (Figs. 4 and 7). Because not enough Sr isotope data are available, the contributions from each source are estimated using the available Pb isotope data. The Pb isotope ratios of the ice core and source-related samples are shown in Fig. 7. This approach allows us to approximately estimate the contributions from natural and anthropogenic sources by using Pb isotopic signatures in the subsamples (Anderson et al., 2002; Chiaradia and Cupelin, 2000). Based on the abundances of ^{206}Pb, ^{207}Pb, and ^{208}Pb measured in the ice core subsamples, the contributions from the three major Pb sources can be apportioned. We obtained an approximate estimate for the contributions from deserts, lead ore and Chinese coal combustion for insoluble dust and the mixed anthropogenic contribution of lead ore, Chinese coal combustion and leaded gasoline for soluble dust using a ternary mixing equation (Cheng and Hu, 2010). Therefore, the Pb sources identified in this study can be divided into four groups: desert dust, which has a low $^{207}Pb/^{206}Pb$ ratio; Chinese coal combustion; lead ore; and leaded gasoline.

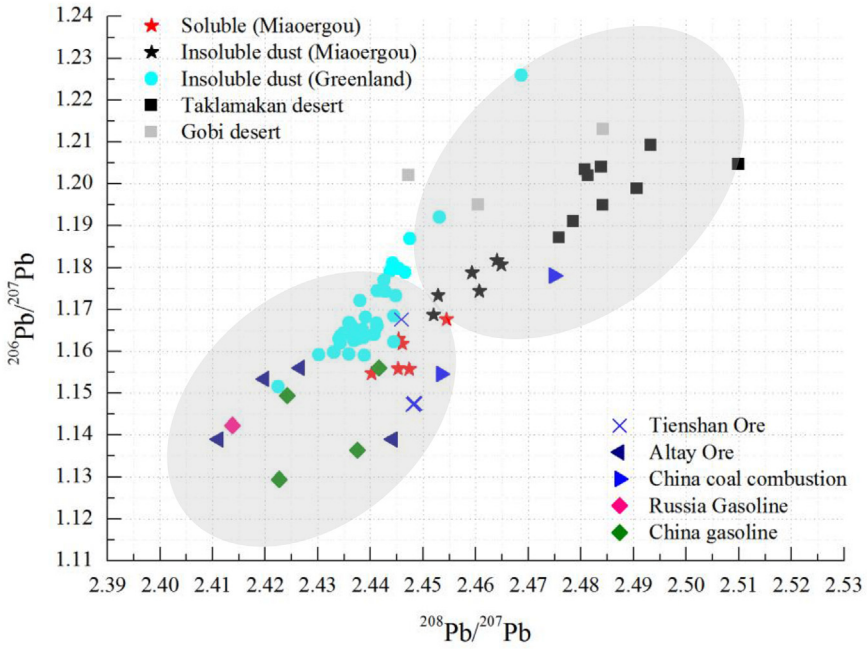

Fig. 7. Lead isotopic compositions of the insoluble dust from the ice of the Miaoergou ice core. In addition, the Pb isotopic ratios of ores from Tian Shan, Kazakhstan and Rudny Altai are shown (Zhu, 1995; Zhang et al., 2010), and the Pb isotopic ratios of samples from the Taklimakan desert, Gobi desert, Russian coal (Biscaye et al., 1997; Mukai et al., 2001; Li, 2007; Bory et al., 2014), leaded vehicle exhaust and gasoline are shown (Mukai et al., 2001; Chen et al., 2005).

$$\left(\frac{^{207}Pb}{^{206}Pb}\right)_{dust} = f_{dust}\left(\frac{^{207}Pb}{^{206}Pb}\right)_{dust} + f_{Ore}\left(\frac{^{207}Pb}{^{206}Pb}\right)_{Ore} + f_{Coal}\left(\frac{^{207}Pb}{^{206}Pb}\right)_{Coal} \quad (1)$$

$$\left(\frac{^{208}Pb}{^{206}Pb}\right)_{dust} = f_{dust}\left(\frac{^{208}Pb}{^{206}Pb}\right)_{dust} + f_{Ore}\left(\frac{^{208}Pb}{^{206}Pb}\right)_{Ore} + f_{Coal}\left(\frac{^{208}Pb}{^{206}Pb}\right)_{Coal} \quad (2)$$

$$f_{Dust} + f_{Ore} + f_{Coal} = 1 \quad (3)$$

$$\left(\frac{^{207}Pb}{^{206}Pb}\right)_{filtrate} = f_{Ore}\left(\frac{^{207}Pb}{^{206}Pb}\right)_{Ore} + f_{Coal}\left(\frac{^{207}Pb}{^{206}Pb}\right)_{Coal} + f_{Gasoline}\left(\frac{^{207}Pb}{^{206}Pb}\right)_{Gasoline} \quad (4)$$

$$\left(\frac{^{208}Pb}{^{206}Pb}\right)_{filtrate} = f_{Ore}\left(\frac{^{208}Pb}{^{206}Pb}\right)_{Ore} + f_{Coal}\left(\frac{^{208}Pb}{^{206}Pb}\right)_{Coal} + f_{Gasoline}\left(\frac{^{208}Pb}{^{206}Pb}\right)_{Gasoline} \quad (5)$$

$$f_{Ore} + f_{Coal} + f_{Gasoline} = 1 \quad (6)$$

where $(^{207}Pb/^{206}Pb)_{dust}$ and $(^{208}Pb/^{206}Pb)_{dust}$ represent the average ratios for insoluble dust; $(^{207}Pb/^{206}Pb)_{filtrate}$ and $(^{208}Pb/^{206}Pb)_{filtrate}$ represent the average ratios for soluble dust; $(^{207}Pb/^{206}Pb)_{Dust}$ and $(^{208}Pb/^{206}Pb)_{Dust}$ represent the average ratios for the Taklamakan and Gobi deserts (0.8330; 2.0650. Li, 2007; Biscaye et al., 1997); $(^{207}Pb/^{206}Pb)_{Ore}$ and $(^{208}Pb/^{206}Pb)_{Ore}$ denote the average ratios for Tienshan and Rudny Altai (0.8700; 2.1150. Zhang et al., 2012; Mukai et al., 2001); $(^{207}Pb/^{206}Pb)_{Coal}$ and $(^{208}Pb/^{206}Pb)_{Coal}$ denote the average ratios for Chinese coal (0.8488, 2.1000. Mukai et al., 1993); and $(^{207}Pb/^{206}Pb)_{Gasoline}$ and $(^{208}Pb/^{206}Pb)_{Gasoline}$ denote the average ratios for Chinese and Russian gasoline (0.8800, 2.1250; Mukai et al., 2001; Yang et al., 2005). The subscripts Dust, Ore, Coal and Gasoline represent the major sources, and fDust, fOre, fCoal and fGasoline represent their relative contributions. The results indicate that the contributions from deserts, lead ore and coal combustion account for approximately 46%, 40% and 14% of the insoluble dust, respectively, and that the contributions from lead ore, coal combustion and leaded gasoline account for approximately 37%, 45% and 18% of the soluble dust, respectively. Therefore, lead ore and Chinese coal combustion are the main sources of pollution for the Miaoergou ice core. Because the ice core is located far from human activities and because gasoline pollution is prominent, these factors may be limited.

4. Conclusions

This study reveals that the Sr and Pb isotopic ratios preserved in an ice core from Miaoergou Glacier represent distinctive geographic characteristics of the ratios between natural aeolian dust provenances and anthropogenic sources. The PSAs were identified with the Sr and Pb isotopic ratios for insoluble dust, originating from the Taklamakan and Gobi deserts. The Pb isotopic ratios of the soluble dust revealed that the ratios changed due to anthropogenic sources, such as lead ore, coal combustion, and leaded gasoline. These results show that the Pb isotopes are well suited as tracers because their ratios exhibit pronounced differences in different media.

Acknowledgments

N. Catto and the anonymous reviewers gave insightful comments of this manuscript. We are grateful to Tong Zhang and A. F. Ali for improving the English and helpful discussions. This research was supported by Ministry of Science and Technology of China (MoST, 2013CBA01804), the National Natural Science Foundation of China (NSFC) (41425003, 41276194) and the Scientific Research Foundation of the Key Laboratory of Cryospheric Sciences (SKLCS-ZZ-2015-01). In addition, we would like to thank all of the field personnel that helped conduct the scientific expedition to the Miaoergou glacier in 2005.

References

Anderson, B.R., Gemmell, J.B., Nelson, D.R., 2002. Lead isotope evolution of mineral deposits in the Proterozoic Throssell Group, Western Australia. Economic Geology 97, 897–911.
Biscaye, P.E., Grousset, F.E., Revel, M., Van der, G.S., Zielinski, G.A., Vaars, A., Kukla, G., 1997. Asian provenance of glacial dust (stage 2) in the Greenland ice sheet Project 2 ice core, Summit, Greenland. Journal of Geophysical Research 102, 26765–26781.
Bollhöfer, A., Rosman, R., 2000. Isotopic source signatures for atmospheric lead: the Southern Hemisphere. Geochimica et Cosmochimica Acta 64, 3251–3262.
Bollhöfer, A., Rosman, K.J.R., 2002. The temporal stability in lead isotopic signatures at selected sites in the Southern and Northern Hemispheres. Geochimica et Cosmochimica Acta 66, 1375–1386.
Bory, A.J.M., Biscaye, P.E., Svensson, A., Grousset, F.E., 2002. Seasonal variability in the origin of recent atmospheric mineral dust at NorthGRIP, Greenland. Earth and Planetary Science Letters 196, 123–134.
Bory, A.J.M., Biscaye, P.E., Grousset, F.E., 2003. Two distinct seasonal Asian source regions for mineral dust deposited in Greenland (NorthGRIP). Geophysical Research Letter 30 (4), 1167. http://dx.doi.org/10.1029/2002GL016446.
Bory, A.J.M., Abouchami, W., Galer, S.J.G., Svensson, A., Christensen, J.N., Biscaye, P.E., 2014. A chinese imprint in insoluble pollutants recently deposited in central greenland as indicated by lead isotopes. Environmental Science and Technology 48, 1451–1457.
Boutron, C.F., Görlach, U., Candelone, J.P., Bolshov, M.A., Delmas, R.J., 1991. Decrease in anthropogenic lead, cadmium and zinc in Greenland snows since the late 1960s. Nature 353, 153–156.
Burton, G.R., Rosman, K.J.R., Candelone, J.P., Burn, L.J., Boutron, C.F., Hong, S.M., 2007. The impact of climatic conditions on Pb and Sr isotopic ratios found in Greenland ice, 7-150 ky BP. Earth and Planetary Science Letters 259, 557–566.
Burn-Nunes, L., Vallelonga, P., Lee, K., Hong, S.M., Burtona, G., Hou, S.H., Moy, A., Edwards, R., Loss, R., Rosman, K., 2014. Seasonal variations in the sources of natural and anthropogenic lead deposited at the East Rongbuk glacier in the high-altitude Himalayas. Science of the Total Environment 487, 407–419.
Chen, J., Tan, M., Li, Y., Zhang, Y., Lu, W., Tong, Y., 2005. A lead isotopic record of Shanghai atmospheric lead emissions in total suspended particles during the period of phasing out of leaded gasoline. Atmospheric Environment 39, 1245–1253.
Cheng, H., Hu, Y., 2010. Lead (Pb) isotopic fingerprinting and its applications in lead pollution studies in China: a review. Environment Pollution 158 (5), 1134–1146.
Chiaradia, M., Cupelin, F., 2000. Behaviour of airborne lead and temporal variations of its source effects in Geneva (Switzerland): comparison of anthropogenic versus natural processes. Atmospheric Environment 34, 959–971.
Cong, Z., Kawamura, K., Kang, S., Fu, P., 2015. Penetration of biomass-burning emissions from South Asia through the Himalayas: new insights from atmospheric organic acids. Scientific Reports 2015 (5), 9580. http://dx.doi.org/10.1038/srep09580.
Delmonte, B., Baroni, C., Andersson, P.S., Narcisi, B., Salvatore, M.C., Petit, J.R., Scarchilli, C., Frezzotti, M., Albani, S., Maggi, V., 2013. Modern and Holocene aeolian dust variability from Talos Dome (Northern Victoria Land) to the interior of the Antarctic ice sheet. Quaternary Science Reviews 64, 76–89.
Dia, A.N., Cohen, A.S., O'Nions, R.K., Shackleton, N.J., 1992. Seawater Sr isotope variation over the past 300 kyr and influence of global climate cycles. Nature 356, 786–788.
Diaz-Somoano, M., Kylander, M.E., Lopez-Znton, M.A., Suarez-Ruiz, I., Martinez-Tarazona, M.R., Ferrat, M., Kober, B., Weiss, D.J., 2009. Stable lead isotope compositions in selected coals from around the world and implications for present day aerosol source tracing. Environmental Science and Technology 43, 1078–1085.
Ding, J., Cheng, X., Zhang, C., Lou, D., Dong, Q., Liu, Y., 2010. Metallogenic rules and regional prediction of lead-Zinc in eastern Tianshan area,China. Geological Bulletin of China 29 (10), 1504–1511.
D'yachkov, B.A., Titov, D.V., Sapargaliev, E.M., 2009. Ore belts of the Greater Altai and their ore resource potential. Geology of Ore Deposits 51 (3), 197–211.
Du, Z., Xiao, C., Liu, Y., Wu, G., 2015. Geochemical characteristics of insoluble dust as a tracer in an ice core from Miaoergou Glacier, East Tienshan. Global and Planetary Change 127, 12–21.

Eichle, A., Tobler, L., Eyrikh, S., Gramlich, G., Malygina, N., Papina, T., Schwikowski, M., 2012. Three centuries of eastern European and Altai lead emissions recorded in a Belukha ice core. Environmental Science and Technology 46, 4323–4330.
Farmer, A., Farmer, M., 2000. Concentration of cadmium, lead and zinc in livestock feed and organs around a metal production center in eastern Kazakhstan. Science of the Total Environment 257, 53–60.
Ferrat, M., Weiss, D.J., Dong, S., Large, D.J., Spiro, B., Sun, Y., Gallagher, K., 2012. Lead atmospheric deposition rates and isotopic trends in Asian dust during the last 9.5 kyr recorded in an ombrotrophic peat bog on the eastern Qinghai Tibetan Plateau. Geochimica et Cosmochimica Acta 82, 4–22.
Grigholm, B., Mayewski, P.A., Kang, S., Aizen, V., Zhang, Y., Zhang, Q., Morgenstern, U., Kaspari, S., Takeuchi, N., Maasch, K., Dixon, D., Birkel, S., Handley, M., Sneed, S., 2015. Twentieth century dust lows and the weakening of the westerly winds over the Tibetan Plateau. Geophysical Research Letter 42, 2434–2441.
Grousset, F.E., Biscaye, P.E., 2005. Tracing dust sources and transport patterns using Sr, Nd and Pb isotopes. Chemical Geology 222, 149–167.
Gross, B., Kreutz, K.J., Osterberg, E., McConnell, J., Handley, M., Wake, C., Yalcin, K., 2012. Constraining recent lead pollution sources in the North Pacific using ice core stable lead isotopes. Journal of Geophysical Research-Atmospheres 117, D16307. http://dx.doi.org/10.1029/2011JD017270.
Grushin, S.P., Papin, D.V., Pozdnykova, O.A., Tujrina, E.A., Fedoruk, A.S., Havrin, S.V., 2009. Altai in the System of Metallurgical Provinces of Aeneolitic and Bronze Age. Publishing House of Altai University, Barnaul, Russia, pp. 122–133 and 157–158.
Hong, S., Candelone, J.P., Patterson, C.C., Boutron, C.F., 1994. Greenland ice evidence of hemispheric lead pollution two millennia ago by Greek and Roman civilizations. Science 265, 1841–1843.
Hong, S., Lee, K., Hou, S., Hur, S.D., Ren, J., Burn, L.J., Rosman, K.J.R., Barbante, D., Boutron, C.F., 2009. An 800-year record of atmospheric As, Mo, Sn, and Sb in central Asia in high-altitude ice cores from Mt. Qomolangma (Everest). Himalayas. Environmental Science and Technology 43, 8060–8065.
Hong, S., Soyol-Erdene, T.O., Hwang, H.J., Hong, S.B., Hur, S.D., Motoyama, H., 2012. Evidence of global-scale As, Mo, Sb and Ti atmospheric pollution in Antarctic Snow. Environmental Science and Technology 46, 11550–11567.
Hur, S.D., Soyol-Erdene, T., Hwang, H.J., Han, C., Gabrielli, P., Barbante, C., Boutron, C.F., Hong, S., 2013. Climate-related variations in atmospheric Sb and Tl in the EPICA Dome C ice (East Antarctica) during the past 800,000 years. Global Biogeochemical Cycles 27, 930–940.
Jitaru, P., Gabrielli, P., Marteel, A., Plane, J.M.C., Planchon, F.A.M., Gauchard, P.A., Ferrari, C.P., Boutron, C.F., Adams, F.C., Hong, S., Cescon, P., Barbante, C., 2009. Atmospheric depletion of mercury over Antarctica during glacial periods. Nature Geoscience 2, 505–508.
Kaspari, S., Mayewski, P.A., Handley, M., Kang, S., Sneed, S., Hou, S., Qin, D., 2009. Recent increases in atmospheric concentrations of Bi, U, Cs, S and Ca from a 350-year Mount Everest ice core record. Journal of Geophysical Research 114 (D4), D04302.
Lambert, F., Delmonte, B., Petit, J.R., Bigler, M., Kaufmann, P.R., Hutterli, M.A., Stocker, T.F., Ruth, U., Steffensen, J.P., Maggi, V., 2008. Dust-climate couplings over the past 800,000 years from the EPICA Dome C ice core. Nature 452, 616–619.
Lee, K., Hur, S.D., Hou, S., Burn-Nunes, L.J., Hong, S., Barbante, C., Boutron, C.F., Rosman, K.J.R., 2011. Isotopic signatures for natural versus anthropogenic Pb in high-altitude Mt. Everest ice cores during the past 800years. Science of the Total Environment 412–413, 194–202.
Li, F., 2007. Distribution characteristics of Lead isotopes in dust source areas and its trace significance in the North of China. Journal of Desert Research 27 (5), 738–744 (in Chinese).
Li, Q., Cheng, H., Zhou, T., Lin, C., Guo, S., 2012. The estimated atmospheric lead emissions in China, 1990-2009. Atmospheric Environment 60, 1–8.
Li, Z., Yao, T., Tian, L., Xu, B., Li, Y., 2006. Atmospheric Pb variations in Central Asia since 1955 from Muztagata ice core record, eastern Pamirs. Chinese Science Bulletin 51, 1996–2000.
Li, Z., Wang, F., Zhu, G., Li, H., 2007a. Basic features of the Miaoergou flat- topped glacier in East Tian Shan Mountains and its thickness change over the past 24 years (in Chinese with English abstract). Journal of Glaciology Geocryology 29 (1), 61–65.
Li, Z., Li, C., Li, Y., Wang, F., Li, H., 2007b. Preliminary results from measurements of selected trace metals in the snow – firn pack on Ürümqi glacier No. 1, eastern Tienshan, China. Journal of Glaciology 53, 368–373.
Liu, D., Zhao, Y., 2006. Ownership, foreign investment and productivity—a case study of the Automotive Industry in China. 2006. No. 21892. East Asian Bureau of Economic Research. JCER Discussion Paper, no. 10.
Liu, Y., Hou, S., Hong, S., Hur, S., Lee, K., Wang, Y., 2011. High-resolution trace element records of an ice core from the eastern Tienshan, central Asia, since 1953 AD. Journal of Geophysical Research 116 (D12), D12307.
Lupker, M., Aciego, S.M., Bourdon, B., Schwander, J., Stocker, T.F., 2010. Isotopic tracing (Sr, Nd, U and Hf) of continental and marine aerosols in an 18th century section of the Dye-3 ice core (Greenland). Earth and Planetary Science Letters 295, 277–286.
Maher, B.A., Prospero, J.M., Mackie, D., Gaiero, D., Hesse, P.P., Balkanski, Y., 2010. Global connections between aeolian dust, climate and ocean biogeochemistry at the present day and at the last glacial maximum. Earth-Science Reviews 99, 61–97.
Marteel, A., Boutron, C.F., Barbante, C., Gabrielli, P., Cozzi, G., Gaspari, V., Cescon, P., Ferrari, C.R., Dommergue, A., Rosman, K., Hong, S.M., Do Hur, S., 2008. Changes in atmospheric heavy metals and metalloids in Dome C (East Antarctica) ice back to 672.0 kyr BP (Marine Isotopic Stages 16.2). Earth and Planetary Sciences Letters 272, 579–590.
McConnell, J.R., Edwards, R., 2008. Coal burning leaves toxic heavy metal legacy in the Arctic. Proceedings of the National Academy of Science of the USA 105 (34), 12140–12144.
Mukai, H., Furuta, N., Fujii, T., Amb, Y., Sakamoto, K., Hashimoto, Y., 1993. Characterization of sources of lead in the urban air of Asia using ratios of stable lead isotopes. Environmental Science and Technology 27, 1347–1356.
Mukai, H., Machida, T., Tanaka, A., Vera, Y.P., Uematsu, M., 2001. Lead isotope ratios in the urban air of eastern and central Russia. Atmospheric Environment 35 (15), 2783–2793.
Nagatsuka, N., Takeuchi, N., Nakano, T., Kokado, E., Li, Z., 2010. Sr, Nd, and Pb stable isotopes of surface dust on Urumqi glacier no. 1 in western China. Annals of Glaciology 51, 95–105.
Nakano, T., Yokoo, Y., Nishikawa, M., Koyanagi, H., 2004. Regional Sr–Nd isotopic ratios of soil minerals in north China as Asian dust fingerprints. Atmospheric Environment 38, 3061–3067.
Negrel, P., Guerrot, C., Millot, R., 2007. Chemical and strontium isotope characterization of rainwater in France: influence of sources and Hydrogeochemical implications. Isotopes in Environmental and Health Studies 43, 179–196.
Osterberg, E., Mayewski, P.A., Kreutz, K.J., Fisher, D.A., Handley, M., Sneed, S., Zdanowicz, C., Zheng, J., Demuth, M., Waskiewicz, M., Bourgeois, J., 2008. Ice core record of rising lead pollution in the North Pacific atmosphere. Geophysical Research Letters 35, L05810.
Qin, J.F., 2010. Estimation of lead emissions to Atmospheric from coal combustion in China, 1953-2005. Guangdong Trace Elements Science 17 (8), 27–35.
Rosman, R., Chisholm, W., Boutron, F., Candelone, P., Görlach, U., 1993. Isotopic evidence for the source of lead in Greenland snows since the late 1960s. Nature 362, 333–334.
Ruth, U., Bigler, M., Röthlisberger, R., Siggaard-Andersen, M.-L., Kipfstuhl, Goto-Azuma, K., Hansson, M., Johnsen, J., Lu, H., Steffensen, J., 2007. Ice core evidence for a very tight link between North Atlantic and East Asian glacial climate. Geophysical Research Letters 34, L03706. http://dx.doi.org/10.1029/2006GL027876.
Svensson, A., Biscaye, P.E., Grousset, F.E., 2000. Characterization of late glacial continental dust in the Greenland Ice Core Project ice core. Journal of Geophysical Research 105 (D4), 4637–4656.
Stracher, G.B., Taylor, T.P., 2004. Coal fires burning out of control around the world: thermodynamic recipe for environmental catastrophe. International Journal of Coal Geology 59 (1–2), 7–17.
Sun, J.M., Zhu, X.K., 2010. Temporal variations in Pb isotopes and trace element concentrations within Chinese eolian deposits during the past 8 Ma: Implications for provenance change. Earth and Planetary Science Letters 290 (3–4), 438–447.
Takahashi, Y., Higashi, M., Furukawa, T., Mitsunobu, S., 2011. Change of iron species and iron solubility in Asian dust during the long-range transport from western China to Japan. Atmospheric Chemistry and Physics 11, 11237–11252.
Thompson, L.G., Yao, T., Thompson, E.M., Davis, M.E., Henderson, K.A., Lin, P.-N., 2000. A high-resolution millennial record of the South Asian monsoon from Himalayan ice cores. Science 289, 1916–1919.
Uno, I., Eguchi, K., Yumimoto, K., Takemura, T., Shimizu, A., Uematsu, M., Liu, Z.Y., Wang, Z.F., Hara, Y., Sugimoto, N., 2009. Asian dust transported one full circuit around the globe. Nature Geoscience 2, 557–560.
Vallelonga, P., Gabrielli, P., Balliana, E., Wegner, A., Delmonte, B., Turetta, C., Burton, G., Vanhaecke, F., Rosman, K.J.R., Hong, S., Boutron, C.F., Cescon, P., Barbante, C., 2010. Lead isotopic compositions in the EPICA Dome C ice core and Southern Hemisphere Potential Source Areas. Quaternary Science Reviews 29, 247–255.
Von Storch, H., Costa-Cabral, M., Hagner, C., Feser, F., Pacyna, J., Pacyna, E., Kolb, S., 2003. Four decades of gasoline lead emissions and control policies in Europe: a retrospective assessment. Science of the Total Environment 311, 151–176.
Widory, D., Liu, X.D., Dong, S.P., 2010. Isotopes as tracers of sources of lead and strontium in aerosols (TSP and $PM_{2.5}$) in Beijing. Atmospheric Environment 44 (30), 3679–3687.
Wu, G., Zhang, C., Zhang, X., Tian, L., Yao, T.D., 2010. Sr and Nd isotopic composition of dust in Dunde ice core, Northern China: Implications for source tracing and use as an analogue of long-range transported Asian dust. Earth and Planetary Science Letters 299, 409–416.
Wu, G., Zhang, C., Xu, B., Mao, R., Joswiak, D., Wang, N., Yao, T., 2013. Atmospheric dust from a shallow ice core from Tanggula: implications for drought in the central Tibetan Plateau over the past 155 years. Quaternary Science Reviews 59, 57–66.
Xu, J., Yu, G., Hou, S., Kang, S., Ren, J., Qin, D., 2012. Sr–Nd isotope evidence for modern aeolian dust sources in mountain glaciers of Western China. Journal of Glaciology 58, 859–865.
Xu, J., Wang, Z., Yu, G., Qin, X., Ren, J., Qin, D., 2014. Characteristics of water soluble ionic species in fine particles from a high altitude site on the northern boundary of Tibetan plateau: mixture of mineral dust and anthropogenic aerosol. Atmospheric Research 143, 43–56.
Yang, H., Duan, G., Liu, C., Tong, X., Lv, H., Duan, R., Mei, Y., Zhang, L., 2005. Determination of lead isotopic ratios in soil and other background samples (Chinese abstract). Chinese Journal of Analytical Chemistry 33 (11), 1603–1606.

Yao, T., Thompson, L., Yang,, W., Yu, W., Gao, Y., Guo,, X., Yang, X., Duan, K., Zhao, H., Xu, B., Pu, J., Lu, A., Xiang, Y., Kattel, D.B., Joswiak, D., 2012. Different glacier status with atmospheric circulations in Tibetan Plateau and surroundings. Nature Climate Change 2, 663–667.

Yokoo, Y., Nakano, T., Nishikawa, M., Quan, H., 2004. Mineralogical variation of Sr–Nd isotopic and elemental compositions in loess and desert and fromthe central Loess Plateau in China as a provenance tracer of wet and dry deposition in the northwestern Pacific. Chemical Geology 204, 45–62.

Yu, G., Xu, J., Kang, S., Zhang, Q., Huang, J., Ren, Q., Ren, J., Qin, D., 2013. Lead isotopic composition of insoluble particles from widespread mountain glaciers in western China: natural vs. Anthropogenic sources. Atmospheric Environment 75, 224–232.

Zhang, S., Zhang, Z., Huang, H., Zhang, D., Xue, C., 2010. Geologic characteristics, Sulfur and Lead isotope study of the Shalitashi Lead-zinc Deposit, southern tianshan (Chinese abstract). Geoscience 24 (05), 856–865.

Zheng, J., Tan, M.G., Shi, Y., Tanaka, A., Li, Y., Zhang, G., Zhang, Y., Shan, Z.C., 2004. Characteristics of lead isotope ratios and elemental concentrations in PM10 fraction of airborne particulate matter in Shanghai after the phase-out of leaded gasoline. Atmospheric Environment 38 (8), 1191–1200.

Zhou, J., Zhuang, X., Alastuey, A., Querol, X., Li, J., 2010. Geochemistry and mineralogy of coal in the recently explored Zhundong large coal field in the Junggar basin, Xinjiang province, China. International Journal of Coal Geology 82, 51–67.

Zhu, L., Tang, J., Lee, B., Zhang, Y., Zhang, F., 2010. Lead concentrations and isotopes in aerosols from Xiamen, China. Marine Pollution Bulletin 60, 1946–1955.